**Preprints of the 21st IFAC World Congress (Virtual)**
**Berlin, Germany, July 12-17, 2020**

# Online Reliability Assessment of Passive Nonlinear Systems Based on Extended State-Observer with Application to Nuclear Reactors

**Zhe Dong*, **, Bowen Li**, Zhiwu Guo*, Chao Guo**, Xiaojin Huang****

**State Key Laboratory of Nuclear Power Safety Monitoring Technology and Equipment,Shenzhen,Guangdong,518172,China*

*** Institute of Nuclear and New Energy Technology, Collaborative Innovation Center of Advanced Nuclear Energy Technology of China, Key Laboratory of Advanced Reactor Engineering and Safety of Ministry of Education, Tsinghua University, Beijing 100084, China (Tel: 86-10-62783764; e-mail: dongzhe@tsinghua.edu.cn).*

**Abstract:** Online reliability assessment based on system model and operational data is crucial for all the safety critical systems. Since system reliability can be calculated directly from failure-rate, the central in online reliability assessment is the determination of failure-rate. In fact, the deviation of actual responses from its expectation can be utilized for disturbance observation which can further determine the failure-rate. In this paper, an extended state observer (ESO) is proposed for general nonlinear dissipative systems, which provides globally bounded observations for not only state-vector but also total disturbance and its differentiation. By assuming that the failure-rate is given by the estimated differentiation of total disturbance, the reliability can be evaluated. This ESO-based online reliability assessment method is then applied to a nuclear heating reactor, and simulation results show the feasibility and effectiveness.

*Keywords:* Online reliability estimation, nonlinear system, extended state-observer, passivity

## 1. INTRODUCTION

Reliability assessment is highly concerned for condition monitoring and maintenance decision, which is meaningful to enhance the operation availability and efficiency of complex engineering systems such as the nuclear plants, chemical processes and aircrafts (Zio, 2009). Usually, reliability estimation can be given by not only the models from physics or experiments but also the condition monitoring (CM) data, where the former leads to the model-based method, and the latter leads to the data-driven method.

Model-based method gives reliability estimations based on the system models either governing failure mechanism or regressed from experiment data. In Di Maio et al. (2015), a multi-state physics model describing the degradation process for nuclear piping systems was proposed, which can be used for mapping the operational condition of nuclear piping systems into discrete states such as no damage, micro-crack, flaw and rupture. In Santhosh et al. (2018), the data from the accelerated life testing based on the samples of instrument and control (I&C) cables was adopted to give a regression model taking the form as an artificial neural network (ANN) for reliability prediction.

Data-driven method is based on the fact that the exacted features of condition monitoring data vary with the degradation process, and can be beneficial when a model is too expensive to be obtained accurately. In Zio et al. (2010), a fuzzy model is proposed for predicting the remaining useful life (RUL) in dynamic failure scenarios, which can be updated online by measurements. In Tao et al. (2018), statistical failure data and condition monitoring (CM) data are combined so as to tune a Bayesian model for dynamic risk assessment. In Zeng et al. (2018), a support vector machine (SVM) based RUL online assessment method is given, where the SVM is regressed by historical data offline, and is updated online by CM data. Similar to Zeng et al. (2018), deep convolution networks are applied for RUL estimation (Li, et al., 2018).

Sometimes, the cost in model regression from historical data is also expensive, especially for safety-critical systems. Since modeling uncertainty can be suppressed online by data, it is meaningful to combine the model-based and data-driven methods for hybrid method. In Baptista, et al. (2019), data-driven methods are coupled with Kalman filtering technique for a higher RUL prediction performance. Further, since the mismatch between actual and expected responses of a given dynamic system is caused by the exterior and interior disturbances, which can directly reflect the deterioration of operation reliability. This mismatch can be estimated by a properly-designed observer combining system model and operation data.

In this paper, an extended state observer (ESO) is given for general nonlinear dissipative systems, which can provide globally bounded estimations for not only state-variables but also the total disturbance and its differentiation. By defining the failure-rate from the differentiation of total disturbance, the system operation reliability can then be calculated directly. This ESO-based reliability estimation method is applied to a nuclear heating reactor (NHR) which is a typical integral pressurized water reactor (iPWR) with a series of advanced design features. After checking the dissipation characteristics of PWR dynamics, numerical simulation results in the cases of normal power maneuver, injection of disturbances and load rejection are given, which show the feasibility and satisfactory performance of this ESO-based reliability estimator.

 

## 2. PROBLEM FORMULATION

Consider nonlinear systems taking the form as

$$\begin{cases}\dot{\boldsymbol{y}}=\boldsymbol{f}_\mathrm{o}(\boldsymbol{y},\boldsymbol{z})+\boldsymbol{G}(\boldsymbol{y})\boldsymbol{u}+\boldsymbol{\xi}\\ \dot{\boldsymbol{z}}=\boldsymbol{f}_\mathrm{i}(\boldsymbol{y},\boldsymbol{z})\end{cases} \tag{1}$$

where

$$\boldsymbol{x}=\begin{bmatrix}\boldsymbol{y}^\mathrm{T} & \boldsymbol{z}^\mathrm{T}\end{bmatrix}^\mathrm{T}\in\mathrm{R}^n, \tag{2}$$

is the state-vector with $\boldsymbol{y}\in\mathrm{R}^m$ measurable and $\boldsymbol{z}\in\mathrm{R}^{n-m}$ unmeasurable, $\boldsymbol{u}\in\mathrm{R}^l$ is the control input, $\boldsymbol{f}_\mathrm{o}\in\mathrm{R}^m$, $\boldsymbol{f}_\mathrm{i}\in\mathrm{R}^{n-m}$ and $\boldsymbol{G}\in\mathrm{R}^{m\times l}$ are given norm-bounded functions, $\boldsymbol{\xi}\in\mathrm{R}^m$ is the total disturbance satisfying

$$\begin{cases}\dot{\boldsymbol{\xi}}=\boldsymbol{\zeta},\\ \dot{\boldsymbol{\zeta}}=\boldsymbol{d},\end{cases} \tag{3}$$

$$\|\boldsymbol{d}\|_2\le D, \tag{4}$$

$\boldsymbol{\xi}$, $\boldsymbol{d}\in\mathrm{R}^m$, and $D$ is a given bounded positive constant.

Furthermore, suppose that nonlinear system (1) is strictly dissipative, i.e. there exists a positive storage function $S(\boldsymbol{x})$ so that

$$\left[\frac{\partial S(\boldsymbol{x})}{\partial\boldsymbol{x}}\right]^\mathrm{T}\boldsymbol{f}(\boldsymbol{x})=-Q(\boldsymbol{x})<0, \tag{5}$$

where

$$\boldsymbol{f}(\boldsymbol{x})=\begin{bmatrix}\boldsymbol{f}_\mathrm{o}^\mathrm{T}(\boldsymbol{y}) & \boldsymbol{f}_\mathrm{i}^\mathrm{T}(\boldsymbol{z})\end{bmatrix}^\mathrm{T}, \tag{6}$$

is also norm-bounded, and function $Q$ is positive-definite.

Total disturbance $\boldsymbol{\xi}$ is mainly induced by the deterioration of process equipment as well as sensors and actuators, which is tightly related to operation reliability $R$ determined by

$$\dot{R}=-r_\mathrm{f}R \tag{7}$$

with $r_\mathrm{f}$ being the failure-rate. Suppose that the failure-rate $r_\mathrm{f}$ is given by the differentiation of total disturbance $\boldsymbol{\zeta}$ through

$$r_\mathrm{f}=\sum_{k=1}^m\left|\mathrm{dz}(\zeta_k,b_k,l_k)\right|, \tag{8}$$

where

$$\mathrm{dz}(\zeta,b,l)=\begin{cases}l(\zeta-b), & \zeta\ge b,\\ 0, & -b<\zeta<b,\\ l(\zeta+b), & \zeta\le -b,\end{cases} \tag{9}$$

is a deadzone function, $b_k$ and $l_k$ are given positive constants. Then, from equations (7) and (8), operation reliability $R$ can be evaluated online by estimating of $\boldsymbol{\xi}$, which leads to the following problem.

## 3. EXTENDED-STATE OBSERVER FOR DISSIPATIVE NONLINEAR SYSTEM

In this section, an extended state-observer (ESO) is newly proposed for nonlinear system (1) satisfying conditions (3), (4) and (5) so as to give a globally bounded estimation of the extended state-vector defined by

$$\boldsymbol{\chi}=\begin{bmatrix}\boldsymbol{x}^\mathrm{T} & \boldsymbol{\xi}^\mathrm{T} & \boldsymbol{\zeta}^\mathrm{T}\end{bmatrix}^\mathrm{T}. \tag{10}$$

The design and performance analysis of the ESO for online-reliability evaluation is summarized as the following theorem, which is the main result of this paper.

**Theorem**. For nonlinear system (1) satisfying conditions (3), (4) and (5), design the corresponding ESO as

$$\begin{cases}\dot{\hat{\boldsymbol{y}}}=\boldsymbol{f}_\mathrm{o}(\hat{\boldsymbol{y}},\hat{\boldsymbol{z}})+\boldsymbol{G}(\boldsymbol{y})\boldsymbol{u}+\hat{\boldsymbol{\xi}}-\varepsilon^{-1}(\boldsymbol{\kappa}+\alpha_1)\boldsymbol{e}_y\\ \dot{\hat{\boldsymbol{z}}}=\boldsymbol{f}_\mathrm{i}(\hat{\boldsymbol{y}},\hat{\boldsymbol{z}})\\ \dot{\hat{\boldsymbol{\xi}}}=-\varepsilon^{-2}\alpha_2\boldsymbol{e}_y+\hat{\boldsymbol{\zeta}}\\ \dot{\hat{\boldsymbol{\zeta}}}=-\varepsilon^{-3}\alpha_3\boldsymbol{e}_y\end{cases} \tag{11}$$

where $\hat{\boldsymbol{y}}$, $\hat{\boldsymbol{z}}$, $\hat{\boldsymbol{\xi}}$ and $\hat{\boldsymbol{\zeta}}$ are respectively the estimations of $\boldsymbol{y}$, $\boldsymbol{z}$, $\boldsymbol{\xi}$ and $\boldsymbol{\zeta}$, $\boldsymbol{K}\in\mathrm{R}^{m\times m}$ is positive-definite and symmetric, function $V$ is the storage function satisfying (5), $\boldsymbol{e}_y=\hat{\boldsymbol{y}}-\boldsymbol{y}$, $\boldsymbol{e}_z=\hat{\boldsymbol{z}}-\boldsymbol{z}$, $\boldsymbol{e}_\xi=\hat{\boldsymbol{\xi}}-\boldsymbol{\xi}$, $\boldsymbol{e}_\zeta=\hat{\boldsymbol{\zeta}}-\boldsymbol{\zeta}$,

$$\boldsymbol{e}_x=\begin{bmatrix}\boldsymbol{e}_y & \boldsymbol{e}_z\end{bmatrix}^\mathrm{T}, \tag{12}$$

and $\alpha_i>0$, $i$=1, 2, 3. ESO (11) can provide globally bounded estimations of state-vector $\boldsymbol{x}$, total disturbance $\boldsymbol{\xi}$ and its variation-rate $\boldsymbol{\zeta}$ if the following conditions are well satisfied:

(A) Algebraic equation

$$s^3+\alpha_1 s^2+\alpha_2 s+\alpha_3=0 \tag{13}$$

is Hurwitz, i.e. every root has a strictly negative real parts.

(B) Storage function $S$ satisfies

$$\frac{\partial S(\boldsymbol{x})}{\partial\boldsymbol{y}}=\boldsymbol{s}(\boldsymbol{y}), \tag{14}$$

$$\frac{\partial^2 S(\boldsymbol{x})}{\partial\boldsymbol{y}^2}=\boldsymbol{T}(\boldsymbol{y}), \tag{15}$$

where $\boldsymbol{T}(\cdot)$ is positive-definite.

**Proof**: From equations (1), (3) and (11), the dynamics of observer error can be written as

$$\begin{cases}\dot{\boldsymbol{e}}_y=\boldsymbol{f}_\mathrm{o}(\boldsymbol{e}_x)+\boldsymbol{h}_\mathrm{o}(\boldsymbol{e}_x,\boldsymbol{x})+\boldsymbol{e}_\xi-\varepsilon^{-1}(\boldsymbol{\kappa}+\alpha_1)\boldsymbol{e}_y\\ \dot{\boldsymbol{e}}_z=\boldsymbol{f}_\mathrm{i}(\boldsymbol{e}_x)+\boldsymbol{h}_\mathrm{i}(\boldsymbol{e}_x,\boldsymbol{x})\\ \dot{\boldsymbol{e}}_\xi=-\varepsilon^{-2}\alpha_2\boldsymbol{e}_y+\boldsymbol{e}_\zeta\\ \dot{\boldsymbol{e}}_\zeta=-\varepsilon^{-3}\alpha_3\boldsymbol{e}_y-\boldsymbol{d}\end{cases} \tag{16}$$

where functions $\boldsymbol{h}_\mathrm{o}(\boldsymbol{e}_x,\boldsymbol{x})$ and $\boldsymbol{h}_\mathrm{i}(\boldsymbol{e}_x,\boldsymbol{x})$ come respectively from the Taylor expansion of functions $\boldsymbol{f}_\mathrm{o}$ and $\boldsymbol{f}_\mathrm{i}$ around $\boldsymbol{e}_x$, i.e.

$$\boldsymbol{f}_\mathrm{a}(\hat{\boldsymbol{x}})=\boldsymbol{f}_\mathrm{a}(\boldsymbol{e}_x+\boldsymbol{x})=\boldsymbol{f}_\mathrm{a}(\boldsymbol{e}_x)+\boldsymbol{h}_\mathrm{a}(\boldsymbol{e}_x,\boldsymbol{x}),\quad \mathrm{a=o,i}. \tag{17}$$

Since $\boldsymbol{f}_\mathrm{o}$ and $\boldsymbol{f}_\mathrm{i}$ are norm-bounded, it can be seen from equations (17) that $\boldsymbol{h}_\mathrm{o}$ and $\boldsymbol{h}_\mathrm{i}$ are norm-bounded. Moreover, define

$$\boldsymbol{h}(\boldsymbol{e}_x,\boldsymbol{x})=\begin{bmatrix}\boldsymbol{h}_\mathrm{o}^\mathrm{T}(\boldsymbol{e}_x,\boldsymbol{x}) & \boldsymbol{h}_\mathrm{i}^\mathrm{T}(\boldsymbol{e}_x,\boldsymbol{x})\end{bmatrix}^\mathrm{T}. \tag{18}$$

Define

$$\tau=t/\varepsilon, \tag{19}$$

and

$$\begin{cases}\bar{\boldsymbol{e}}_\xi=\varepsilon\boldsymbol{e}_\xi,\\ \bar{\boldsymbol{e}}_\zeta=\varepsilon^2\boldsymbol{e}_\zeta.\end{cases} \tag{20}$$

Then error dynamics can be rewritten as

$$\frac{\mathrm{d}}{\mathrm{d}\tau}\begin{bmatrix}\boldsymbol{e}_y\\ \boldsymbol{e}_z\\ \bar{\boldsymbol{e}}_\xi\\ \bar{\boldsymbol{e}}_\zeta\end{bmatrix}=\begin{bmatrix}\varepsilon\left[\boldsymbol{f}_\mathrm{o}(\boldsymbol{e}_x)+\boldsymbol{h}_\mathrm{o}(\boldsymbol{e}_x,\boldsymbol{x})\right]+\bar{\boldsymbol{e}}_\xi-(\boldsymbol{\kappa}+\alpha_1)\boldsymbol{e}_y\\ \varepsilon\left[\boldsymbol{f}_\mathrm{i}(\boldsymbol{e}_x)+\boldsymbol{h}_\mathrm{i}(\boldsymbol{e}_x,\boldsymbol{x})\right]\\ -\alpha_2\boldsymbol{e}_y+\bar{\boldsymbol{e}}_\zeta\\ -\alpha_3\boldsymbol{e}_y-\varepsilon^3\boldsymbol{d}\end{bmatrix}. \tag{21}$$

Choose the Lyapunov function of error dynamics (21) as

$$V(\boldsymbol{e}_x,\boldsymbol{e}_\xi,\boldsymbol{e}_\zeta)=S(\boldsymbol{e}_x)+\frac{1}{2}\sum_{k=1}^m\bar{\boldsymbol{e}}_k^\mathrm{T}\boldsymbol{P}\bar{\boldsymbol{e}}_k, \tag{22}$$

where

$$\bar{\boldsymbol{e}}_k=\begin{bmatrix} e_{y,k} & \varepsilon e_{\xi,k} & \varepsilon^2 e_{\zeta,k}\end{bmatrix}^{\mathrm{T}},\quad k=1,\cdots,m, \tag{23}$$

$e_{y,k}$, $e_{\xi,k}$ and $e_{\zeta,k}$ are respectively the $k$th element of $\boldsymbol{e}_y$, $\boldsymbol{e}_\xi$ and $\boldsymbol{e}_\zeta$. Further, define

$$\bar{\boldsymbol{e}}=\begin{bmatrix}\bar{\boldsymbol{e}}_1^{\mathrm{T}} & \bar{\boldsymbol{e}}_2^{\mathrm{T}} & \cdots & \bar{\boldsymbol{e}}_m^{\mathrm{T}}\end{bmatrix}^{\mathrm{T}}, \tag{24}$$

$$\bar{\boldsymbol{e}}_y=\begin{bmatrix}\boldsymbol{e}_y^{\mathrm{T}} & \boldsymbol{e}_\xi^{\mathrm{T}} & \boldsymbol{e}_\zeta^{\mathrm{T}}\end{bmatrix}^{\mathrm{T}}, \tag{25}$$

Then, it can be seen that

$$\bar{\boldsymbol{e}}=\boldsymbol{U}\bar{\boldsymbol{e}}_y \tag{26}$$

where $\boldsymbol{U}$ is an orthogonal matrix given by

$$\boldsymbol{U}=\begin{bmatrix}\boldsymbol{U}_1^{\mathrm{T}} & \cdots & \boldsymbol{U}_m^{\mathrm{T}}\end{bmatrix}^{\mathrm{T}},\quad \boldsymbol{U}_k=\boldsymbol{I}_3\otimes\boldsymbol{\upsilon}_k,, \tag{27}$$

$$\boldsymbol{\upsilon}_k=\begin{bmatrix}\upsilon_{k,i}\end{bmatrix}_{1\times m}\quad \upsilon_{k,i}=\begin{cases}1, & i=k,\\ 0, & i\neq k.\end{cases} \tag{28}$$

Differentiate function $V$ along the trajectory of (21),

$$\begin{aligned}\frac{\mathrm{d}V}{\mathrm{d}\tau}&=\varepsilon\left[\frac{\partial S(\boldsymbol{e}_x)}{\partial \boldsymbol{e}_x}\right]^{\mathrm{T}}\left[\boldsymbol{f}(\boldsymbol{e}_x)+\boldsymbol{h}(\boldsymbol{e}_x,\boldsymbol{x})\right]\\ &+\boldsymbol{s}^{\mathrm{T}}(\boldsymbol{e}_y)\left[\bar{\boldsymbol{e}}_\xi-(\kappa+\alpha_1)\boldsymbol{e}_y\right]\\ &+\frac{1}{2}\sum_{k=1}^{m}\bar{\boldsymbol{e}}_k^{\mathrm{T}}\left(\boldsymbol{A}^{\mathrm{T}}\boldsymbol{P}+\boldsymbol{P}\boldsymbol{A}\right)\bar{\boldsymbol{e}}_k+\varepsilon\bar{\boldsymbol{e}}_y^{\mathrm{T}}\boldsymbol{U}^{\mathrm{T}}\boldsymbol{P}\boldsymbol{U}\boldsymbol{\eta}(\boldsymbol{e}_x,\boldsymbol{d}),\end{aligned} \tag{29}$$

where

$$\boldsymbol{\eta}(\boldsymbol{e}_x,\boldsymbol{d})=\begin{bmatrix}\boldsymbol{f}_{\mathrm{o}}(\boldsymbol{e}_x)+\boldsymbol{h}_{\mathrm{o}}(\boldsymbol{e}_x,\boldsymbol{x})\\ \boldsymbol{O}\\ \varepsilon^2\boldsymbol{d}\end{bmatrix}, \tag{30}$$

$$\boldsymbol{A}=\begin{bmatrix}-\alpha_1 & 1 & 0\\ -\alpha_2 & 0 & 1\\ -\alpha_3 & 0 & 0\end{bmatrix}, \tag{31}$$

$$\bar{\boldsymbol{P}}=\boldsymbol{I}_m\otimes\boldsymbol{P}. \tag{32}$$

Since algebraic equation (13) is Hurwitz, matrix $\boldsymbol{A}$ is strictly negative-definite, which is equivalent to the fact that for arbitrary positive-definite matrix $\boldsymbol{Q}$, there exists $\boldsymbol{P}$ so that

$$\boldsymbol{A}^{\mathrm{T}}\boldsymbol{P}+\boldsymbol{P}\boldsymbol{A}=-\boldsymbol{Q}. \tag{33}$$

Moreover, from conditions (14) and (15),

$$\boldsymbol{s}(\boldsymbol{e}_y)=\boldsymbol{T}(\boldsymbol{e}_y)\boldsymbol{e}_y+\boldsymbol{o}\left(\|\boldsymbol{e}_y\|_2\right), \tag{34}$$

which further shows that

$$\begin{cases}\boldsymbol{s}^{\mathrm{T}}(\boldsymbol{e}_y)\boldsymbol{e}_y=\gamma\|\boldsymbol{e}_y\|_2^2,\\ \|\boldsymbol{s}(\boldsymbol{e}_y)\|_2^2=\theta\|\boldsymbol{e}_y\|_2^2,\end{cases} \tag{35}$$

where $\gamma$ and $\theta$ are positive constants, and $\boldsymbol{o}(\cdot)$ denotes the high order terms. Substitute (33), (34) and (35) to (29),

$$\begin{aligned}\frac{\mathrm{d}V}{\mathrm{d}\tau}&\leq-\varepsilon Q(\boldsymbol{e}_x)-\frac{1}{4}\bar{\boldsymbol{e}}_y^{\mathrm{T}}\boldsymbol{U}^{\mathrm{T}}\bar{\boldsymbol{Q}}\boldsymbol{U}\boldsymbol{e}_y\\ &-\left(\alpha_1+\frac{\kappa}{2}\right)\gamma\|\boldsymbol{e}_y\|_2^2+\frac{\varepsilon^2\theta^2}{2\kappa\gamma}\|\boldsymbol{e}_\xi\|_2^2\\ &+\varepsilon^2\boldsymbol{\eta}^{\mathrm{T}}(\boldsymbol{e}_x,\boldsymbol{d})\boldsymbol{U}\bar{\boldsymbol{P}}^{\mathrm{T}}\left(\boldsymbol{U}^{\mathrm{T}}\bar{\boldsymbol{Q}}\boldsymbol{U}\right)^{-1}\bar{\boldsymbol{P}}\boldsymbol{U}\boldsymbol{\eta}(\boldsymbol{e}_x,\boldsymbol{d}),\end{aligned} \tag{36}$$

where

$$\bar{\boldsymbol{Q}}=\boldsymbol{I}_m\otimes\boldsymbol{Q}. \tag{37}$$

From (36), the estimation error converge globally asymptotically to a bounded neighborhood of origin which is tighter if scaling factor $\varepsilon$ is smaller. This completes the proof.

**Remark 1.** Usually it is easy to choose positive constants $\alpha_i$ ($i$=1, 2, 3) so that condition (A) can be satisfied. The difficulty in applying ESO (11) is to check dissipation condition (5) and condition (B) given by (14) and (15). For mechanical, electrical and electromechanical systems, total energy can be adopted as the storage function. For thermodynamic systems, energy cannot be feasible, and shifted-ectropy is usually used to construct storage functions.

**Remark 2.** From equations (7), (11) and (8), the operational reliability can be estimated by

$$\hat{R}(t)=e^{-\int_0^t\hat{r}_{\mathrm{f}}(\tau)\mathrm{d}\tau}=e^{-\int_0^t\left[\sum_{k=1}^{m}\left|\mathrm{dz}\left(\hat{\zeta}_k(\tau),b_k,l_k\right)\right|\right]\mathrm{d}\tau}. \tag{38}$$

Moreover, based on the relationship between failure-rate and lifetime, the RUL $L(t)$ is given by

$$\hat{L}(t)=L_0-\int_0^t\tau\hat{r}_{\mathrm{f}}(\tau)\mathrm{d}\tau=L_0-\int_0^t\left[\sum_{k=1}^{m}\left|\mathrm{dz}\left(\hat{\zeta}_k(\tau),b_k,l_k\right)\right|\right]\mathrm{d}\tau, \tag{39}$$

where $L_0$ is the initial useful life.

## 4. APPLICATION TO NUCLEAR REACTORS

In this section, ESO (11) is applied to evaluate the operation reliability of general pressurized water reactors (PWRs). Based on giving the dynamic model, both dissipation condition (11) and condition (B) given by (14) and (15) are verified, and the expression of a special ESO for PWRs is given.

### *4.1 State-Space Model*

The PWR dynamic model for ESO design is the point kinetics with one equivalent delayed neutron group and temperature feedback from both the fuel and coolant temperature, which is given as follows [29, 6-8]:

$$\begin{cases}\dot{n}_{\mathrm{r}}=-\dfrac{\beta}{\Lambda}(n_{\mathrm{r}}-c_{\mathrm{r}})+\dfrac{n_{\mathrm{r}}\rho_{\mathrm{r}}}{\Lambda}+\dfrac{n_{\mathrm{r}}}{\Lambda}\left[\alpha_{\mathrm{f}}\left(T_{\mathrm{f}}-T_{\mathrm{f,m}}\right)+\alpha_{\mathrm{c}}\left(T_{\mathrm{cav}}-T_{\mathrm{cav,m}}\right)\right],\\ \dot{c}_{\mathrm{r}}=\lambda(n_{\mathrm{r}}-c_{\mathrm{r}}),\\ \dot{T}_{\mathrm{f}}=\dfrac{1}{\mu_{\mathrm{f}}}\left[\gamma_{\mathrm{f}}P_0n_{\mathrm{r}}-\Omega(T_{\mathrm{f}}-T_{\mathrm{cav}})\right],\\ \dot{T}_{\mathrm{cav}}=\dfrac{1}{\mu_{\mathrm{c}}}\left[(1-\gamma_{\mathrm{f}})P_0n_{\mathrm{r}}+\Omega(T_{\mathrm{f}}-T_{\mathrm{cav}})-2M(T_{\mathrm{cav}}-T_{\mathrm{cin}})\right],\end{cases} \tag{40}$$

where $n_{\mathrm{r}}$ and $c_{\mathrm{r}}$ are respectively the normalized neutron flux and concentration of delayed neutron precursor, $\beta$ is the fraction of delayed neutrons, $\Lambda$ is the effective lifetime of prompt neutron, $\lambda$ is the decay constant of delayed neutron precursor, $T_{\mathrm{f}}$ is the average fuel temperature, $T_{\mathrm{cav}}$ and $T_{\mathrm{cin}}$ are the average and inlet primary coolant temperatures respectively, $T_{\mathrm{f,m}}$ and $T_{\mathrm{cav,m}}$ are the initial equilibrium values corresponding to $T_{\mathrm{f}}$ and $T_{\mathrm{cav}}$ respectively, $\alpha_{\mathrm{f}}$ and $\alpha_{\mathrm{c}}$ are the reactivity feedback coefficients of the fuel and coolant temperatures respectively, $\Omega$ is the heat transfer coefficient between fuel and coolant, $M$ is the mass flow rate times heat capacity of the primary coolant, $P_0$ is the rated thermal power, $\rho_{\mathrm{r}}$ is the exterior reactivity, $\mu_{\mathrm{f}}$ is the total heat capacity of fuel, $\mu_{\mathrm{c}}$ is the total heat capacity of primary coolant, $\gamma_{\mathrm{f}}$ is the fraction of reactor power deposited in the fuel, and $0<\gamma_f<1$. Here, it is not loss of generality to suppose that both $\alpha_f$ and $\alpha_c$ are strictly negative.

Let $n_{r0}$, $c_{r0}$, $T_{f0}$, $T_{cav0}$, $T_{cin0}$ and $\rho_{r0}$ be respectively the expected steady values of $n_r$, $c_r$, $T_f$, $T_{cav}$, $T_{cin}$ and $\rho_r$. Define the deviations as $\delta n_r=n_r-n_{r0}$, $\delta c_r=c_r-c_{r0}$, $\delta T_f=T_f-T_{f0}$, $\delta T_{cav}=T_{cav}-T_{cav}$, $T_{cin}=T_{cin}-T_{cin0}$ and $\delta\rho_r=\rho_r-\rho_{r0}$.

Choose

$$\begin{cases} \boldsymbol{x}=\left[x_i\right]_{1\times 4}=\left[\delta n_r \quad \delta T_{cav} \quad \delta c_r \quad \delta T_f\right]^{\mathrm{T}}, \\ \boldsymbol{y}=\boldsymbol{C}\boldsymbol{x}, \\ \boldsymbol{\xi}=\left[\Lambda^{-1}\left(n_{r0}+x_1\right)\delta\rho_r \quad 2\mu_c^{-1}M\delta T_{cin}\right]^{\mathrm{T}}, \end{cases} \tag{41}$$

where

$$\boldsymbol{C}=\left[\boldsymbol{I}_2 \quad \boldsymbol{O}_2\right]. \tag{42}$$

Then, the state-space model of PWRs can be written as

$$\dot{\boldsymbol{x}}=\boldsymbol{f}\left(\boldsymbol{x}\right)+\boldsymbol{C}^{\mathrm{T}}\boldsymbol{\xi} \tag{43}$$

where

$$\boldsymbol{f}\left(\boldsymbol{x}\right)=\begin{bmatrix} -\Lambda^{-1}\beta\left(x_1-x_3\right)+\Lambda^{-1}\left(n_{r0}+x_1\right)\left(\alpha_c x_2+\alpha_f x_4\right) \\ \mu_c^{-1}\left(1-\gamma_f\right)P_0 x_1-\mu_c^{-1}\Omega\left(x_2-x_4\right)-2\mu_c^{-1}Mx_2 \\ \lambda\left(x_1-x_3\right) \\ \mu_f^{-1}\Omega\left(x_2-x_4\right)+\mu_f^{-1}\gamma_f P_0 x_1 \end{bmatrix}. \tag{44}$$

### 4.2 *Verification of Conditions*

To apply ESO (11) for online operational reliability analysis, it is central to verify that PWR dynamics (43) is strictly dissipative under a proper storage function. The verification of dissipativity is summarized as the following proposition.

**Proposition.** PWR dynamics (43) with negative temperature reactivity feedback coefficients $\alpha_f$ and $\alpha_c$ is strictly dissipative under storage function $S$ given by

$$S\left(\boldsymbol{x}\right)=\left[\Lambda x_1+\frac{\beta}{\lambda}x_3-n_{r0}\ln\left(1+\frac{x_1}{n_{r0}}\right)^{\Lambda}\left(1+\frac{x_3}{n_{r0}}\right)^{\frac{\beta}{\lambda}}\right] -\frac{1}{2P_0}\left(\frac{\alpha_c\mu_c}{1-\gamma_f}x_2^2+\frac{\alpha_f\mu_f}{\gamma_f}x_4^2\right), \tag{45}$$

if inequality

$$\left[1-\frac{\alpha_c\gamma_f}{\alpha_f\left(1-\gamma_f\right)}\right]^2<\frac{8M\alpha_c\gamma_f}{\Omega\alpha_f\left(1-\gamma_f\right)} \tag{46}$$

is well satisfied.

**Proof:** Since both $\alpha_f$ and $\alpha_c$ are strictly negative, function $S(\boldsymbol{x})$ is strictly positive definite. Moreover, from (46), there is a positive constant $\sigma\in(0, 1)$ so that

$$\left[1-\frac{\alpha_c\gamma_f}{\alpha_f\left(1-\gamma_f\right)}\right]^2=\frac{8\sigma M\alpha_c\gamma_f}{\Omega\alpha_f\left(1-\gamma_f\right)} \tag{47}$$

From dissipation condition (5), it can be derived that

$$\left(\frac{\partial S}{\partial\boldsymbol{x}}\right)^{\mathrm{T}}\boldsymbol{f}=-\frac{\beta\left(x_1-x_3\right)^2}{\left(n_{r0}+x_1\right)\left(n_{r0}+x_3\right)}+\frac{\alpha_f\Omega}{\gamma_f P_0}\left[x_4^2-x_2x_4 -\frac{\gamma_f}{1-\gamma_f}\cdot\frac{\alpha_c}{\alpha_f}\left(\left(1+\frac{2M}{\Omega}\right)x_4^2-x_2x_4\right)\right]. \tag{48}$$

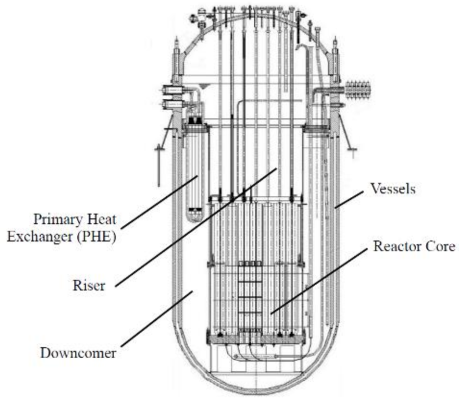


*Fig. 1. The schematic diagram of NHR.*

From equations (47) and (48), dissipation condition (5) is satisfied with $Q$ given by

$$Q\left(\boldsymbol{x}\right)=\frac{\beta\left(x_1-x_3\right)^2}{\left(n_{r0}+x_1\right)\left(n_{r0}+x_3\right)}-\frac{2\left(1-\sigma\right)\alpha_c M}{\left(1-\gamma_f\right)P_0}x_4^2 -\frac{\alpha_f\Omega}{\gamma_f P_0}\left[x_4-\frac{1}{2}\left(1+\frac{\gamma_f}{1-\gamma_f}\cdot\frac{\alpha_c}{\alpha_f}\right)x_2\right]^2>0, \tag{49}$$

which completes the proof of this proposition. Moreover, it can be also verified that

$$\frac{\partial S\left(\boldsymbol{x}\right)}{\partial\boldsymbol{y}}=\left[\frac{\Lambda x_1}{n_{r0}+x_1} \quad \frac{\alpha_c\mu_c}{\left(1-\gamma_f\right)P_0}x_2\right]^{\mathrm{T}}=\boldsymbol{s}\left(y\right), \tag{50}$$

$$\frac{\partial^2 S\left(\boldsymbol{x}\right)}{\partial\boldsymbol{y}^2}=\mathrm{diag}\left(\left[\frac{\Lambda n_{r0}}{\left(n_{r0}+x_1\right)^2} \quad \frac{\alpha_c\mu_c}{\left(1-\gamma_f\right)P_0}\right]\right)=\boldsymbol{T}\left(x_1\right)>0. \tag{51}$$

From (50), (51) and the above proposition, it can be seen that ESO can be applied to PWRs satisfying (46) for online reliability estimation.

### 4.3 *ESO for PWRs*

From state-space model of PWRs (43), it can be seen that m=2, and then the ESO for PWRs can be given as

$$\begin{cases} \dot{\hat{\boldsymbol{x}}}=\boldsymbol{f}\left(\hat{\boldsymbol{x}}\right)+\boldsymbol{C}^{\mathrm{T}}\left[\hat{\boldsymbol{\xi}}-\varepsilon^{-1}\left(\kappa+\alpha_1\right)\boldsymbol{e}_y\right], \\ \dot{\hat{\boldsymbol{\xi}}}=-\varepsilon^{-2}\alpha_2\boldsymbol{e}_y+\hat{\boldsymbol{\zeta}}, \\ \dot{\hat{\boldsymbol{\zeta}}}=-\varepsilon^{-3}\alpha_3\boldsymbol{e}_y, \end{cases} \tag{52}$$

where

$$\boldsymbol{e}_y=\left[\hat{x}_1-x_1 \quad \hat{x}_2-x_2\right]^{\mathrm{T}} \tag{53}$$

$\hat{\boldsymbol{\xi}}$, $\hat{\boldsymbol{\zeta}}\in\mathrm{R}^2$, and positive constants $\alpha_i$ ($i$ =1, 2, 3) satisfy condition (A) in the theorem.

## 5. SIMULATION RESULTS AND DISCUSSIONS

In this section, ESO of PWRs given by (52) is applied to the online operational reliability estimation of a nuclear heating reactor (NHR) that is a typical integral pressurized water reactor (iPWR) with a series of advanced features such as the integral primary circuit, full-power-range natural circulation, self-pressurization, passive removal of residual heat and hydraulically control rod driving (Dong, Pan, 2019). The schematic diagram of NHR with a rated thermal power of 200MW$_{th}$ is shown in following Fig. 1. The cold water leaving from the primary side of primary heat exchangers (PHEs) enters to the reactor core from its bottom, which is then heated up by the fission power. The output hot water flows upward along the riser, and enters to the primary sides of PHEs so as to transfer its heat to the secondary coolant. The primary circulation is naturally driven by coolant density difference. The secondary coolant flows of PHEs combine together to form two intermittent circuits (ICs) each of which drives a U-tube steam generator (UTSG) for power generation or heat supply.

### *5.1 Simulation Results*

In this numerical simulation, ESO (52) is applied to estimate the unmeasurable states and disturbances so as to evaluate its operation reliability of NHR online by equation (38). The parameters of ESO are chosen as $\alpha_1=3a$, $\alpha_2=3a^2$, $\alpha_3=a^3$, $a=1$, $\kappa=1$ and $\varepsilon=0.01$, and the parameters of failure-rates are chosen as $b_1=0.005$, $b_2=0.05$ and $l_1=l_2=1$. To verify the feasibility and to show the performance, the following cases are considered, where the initial condition is that the NHR steadily operates at its full power (FP).

A. Normal power maneuver

The setpoint of NHR thermal power start at 3000s to decrease from 100% to 20%FP in a rate of 20%FP/min, and the responses of key variables are shown in Fig. 2.

B. Disturbance of reactivity

A step decrease of reactivity with the amount of 0.2$ occurs at 3000s, and the responses are shown in Fig. 3.

C. Disturbance of IC flowrate

A step decrease of IC flow with an amplitude of 200kg/s occurs at 3000s. The responses are shown in Fig. 4.

D. Load Reject

At 3000s, the setpoint of thermal power steps down from 100% to 40% FP, and the responses are shown in Fig. 5.

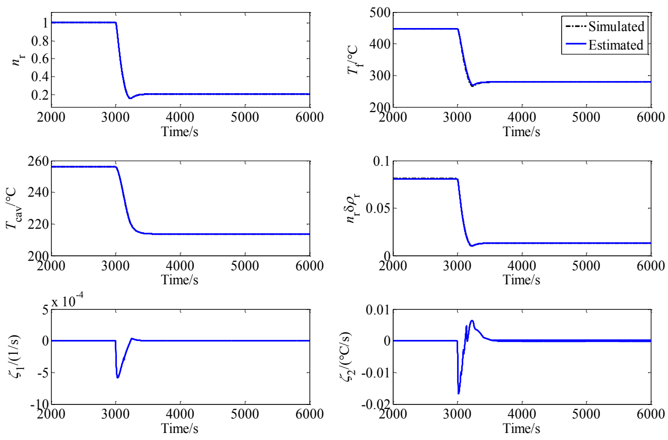


*Fig. 2. Reponses in Case A, $n_r$: normalized neutron flux, $T_f$: averaged fuel temperature, $T_{cav}$: averaged temperature of primary coolant, $n_r\delta\rho_r=\xi_1$.*

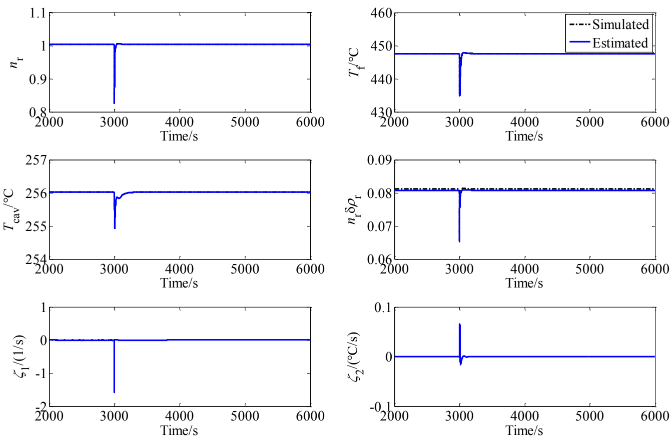


*Fig. 3. Reponses in Case B, $n_r$: normalized neutron flux, $T_f$: averaged fuel temperature, $T_{cav}$: averaged temperature of primary coolant, $n_r\delta\rho_r=\xi_1$.*

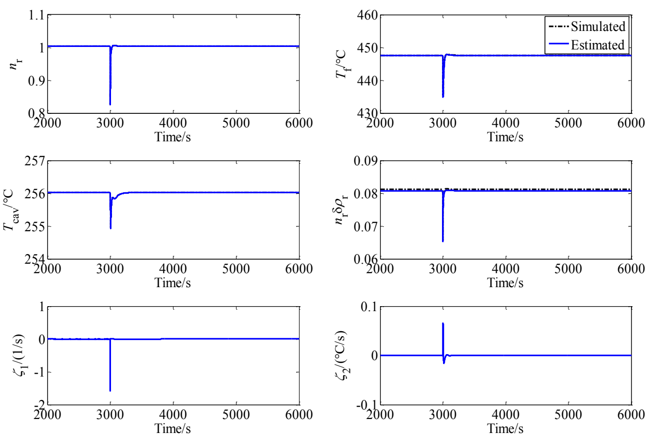


*Fig. 4. Reponses in Case C, $n_r$: normalized neutron flux, $T_f$: averaged fuel temperature, $T_{cav}$: averaged temperature of primary coolant, $n_r\delta\rho_r=\xi_1$.*

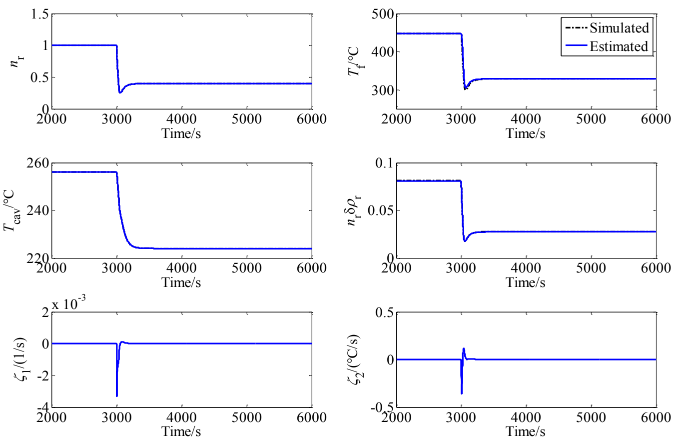


*Fig. 5. Reponses in Case D, $n_r$: normalized neutron flux, $T_f$: averaged fuel temperature, $T_{cav}$: averaged temperature of primary coolant, $n_r\delta\rho_r=\xi_1$.*

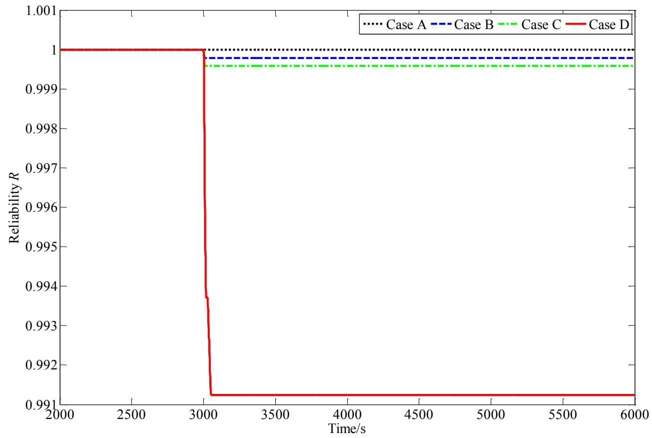


*Fig.6. Deterioration of reactor operational reliability in cases A, B, C and D.*

### *5.2 Discussions*

From Figs. 2-5, we can see that ESO (52) for PWRs can give satisfactory observation for the unmeasurable state-variables as well as disturbances. The reactor reliability deterioration calculated by equation (38) based upon the disturbance observation provided by ESO (52) is shown in Fig. 6, from which it can be seen that there exists reliability deterioration in all the cases except case A. From the responses of cases B-D shown in Figs. 3-5, disturbance injections and load rejections can induce larger overshoots of state variables $\zeta_1$ and $\zeta_2$ which surpasses the limitation of deadzone function and induces reliability deterioration. Since the load rejection triggers the fast and large-range variations of all the process variables, the reliability decrease in case D is much larger than those in cases B and C. Based on the above discussion, the ESO-based operation reliability estimation method is feasible for the online evaluation of reliability of nuclear reactors. It is easy to implement ESO (52) on the digital control system platforms, which shows that the method proposed in this paper is deployable.

## 6. CONCLUSIONS

The mismatch between the desired and actual responses of a dynamical system can be adopted to estimate the corresponding total disturbance and its differentiation that can be utilized for operational reliability evaluation. In this paper, a novel ESO is proposed for general nonlinear dissipative systems which can provide globally bounded estimations for the state-variables as well as the total disturbance and its differentiation. Then, the evaluation of system operational reliability is given based on the failure-rate defined on the estimated differentiation of total disturbance. To verify this ESO-based reliability evaluation method, it is applied to a NHR. After checking the dissipativity of general PWRs, numerical simulation results in the cases of normal power operation, injections of reactivity and IC flowrate disturbances as well as load rejection are all given, and the reactivity deterioration in the four cases are also shown, which strongly show the feasibility and satisfactory performance of the ESO-based reliability estimation method.

## ACKNOWLEDGMENT

This work is jointly supported by National S&T Major Project of China (Grant No.ZX069) and Natural Science Foundation of China (Grant No.61773228).

## REFERENCES

Baptista, M., Henriqes, E.M.P., De Medeiros, I.P., et al. (2019). Remaining useful life estimation in aeronaustics: combining data-driven and Kalman filtering. *Reliability Engineering & System Safety*, 184, 228-239.

Di Maio, F., Colli, D., Zio, E., Liu, T., Tong, J. (2015). A multi-state physics modeling approach for the reliability assessment of nuclear power plants piping systems. *Annals of Nuclear Energy*, 80, 151-65.

Dong, Z., Pan, Y. (2018). A lumped-parameter dynamical model of a nuclear heating reactor cogeneration plant. *Energy*, 145, 638-56.

Li, X., Ding Q., Sun, J.-Q. (2018). Remaining useful life estimation in prognostics using deep convolution neural networks. *Reliability Engineering & System Safety*, 172, 1-11.

Santhosh, T.V., Gopika, V., Ghosh, A.K., Fernandes, B.G. (2018). An approach for reliability prediction of instrumentation & control cables by artificial neural networks and Weibull theory for probabilistic safety assessment of NPPs. *Reliability Engineering and System Safety*, 170, 31-44.

Tao, T., Zio, E., Zhao, W. (2018). A novel support vector regression method for online reliability prediction under multi-state varying operating condtions. *Reliability Engineering & System Safety*, 177, 35-49.

Zeng, Z., Zio E. (2018). Dynamic risk assessment based on statistical failure data and condition-monitoring degration data. *IEEE Transactions on Reliability*, 67, 609-22.

Zio, E. (2009). Reliability engineering: old problems and new challenges. *Reliability Engineering and System Safety*, 94, 125-141.

Zio, E., Di Maio, F. (2010). A data-driven fuzzy approach for predicting the remaining useful life in dynamic failure senerios of a nuclear system. *Reliability Engineering & System Safety*, 95, 49-57.